

## Supporting information

for

# Tuning the magnetic properties of graphene derivatives by functional group selection

Rostislav Langer<sup>b</sup>, Piotr Błoński<sup>a\*</sup>, Michal Otyepka<sup>a,b\*</sup>

<sup>a</sup> Regional Centre of Advanced Technologies and Materials, Faculty of Science, Palacký University in Olomouc, Šlechtitelů 27, 783 71 Olomouc, Czech Republic.

<sup>b</sup> Department of Physical Chemistry, Faculty of Science, Palacký University in Olomouc, tř. 17, listopadu 12, 771 46 Olomouc, Czech Republic

\*Email: piotr.blonski@upol.cz, michal.otyepka@upol.cz

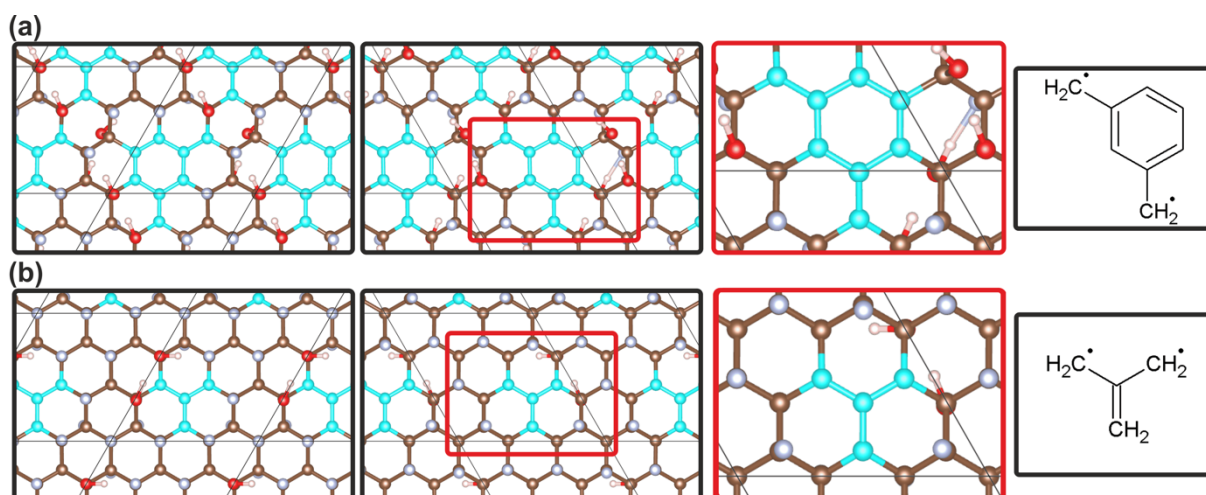


**Fig. S1** Models of G(OH)F systems with embedded diradical motifs. (a) *m*-xylylene motifs (MX) embedded in C<sub>18</sub>(OH)<sub>4</sub>F<sub>6</sub> and (b) trimethylenemethane motifs (TMM) embedded in C<sub>18</sub>(OH)<sub>2</sub>F<sub>12</sub>. The left/middle panels show the diradical motifs from above/below the graphene plane, the right panels focus on the diradical motifs. The insets show the chemical structures of the two diradical motifs. Fluorine atoms are shown in bluish, hydrogen atoms in white, oxygen atoms in red, *sp*<sup>3</sup> carbon atoms in brown, and *sp*<sup>2</sup> carbon atoms in turquoise.

**Table S1** Stability of C<sub>18</sub>(X)<sub>4</sub>F<sub>6</sub> with *m*-xylylene motif and C<sub>18</sub>(X)<sub>2</sub>F<sub>12</sub> with trimethylenemethane motif calculated for FM ground-state in terms of cohesive energy per atom  $E_{coh}$  (eV)

$E_{coh}$ (eV)	OH	NH <sub>2</sub>	CH <sub>3</sub>	BH <sub>3</sub>	BH <sub>2</sub>	F
C <sub>18</sub> (X) <sub>4</sub> F <sub>6</sub>	-5.73	-5.39	-5.35	-5.15 (NM)	-5.52 (NM)	-5.92
C <sub>18</sub> (X) <sub>2</sub> F <sub>12</sub>	-5.45	-5.30	-5.30	-5.14	-5.35	-5.52

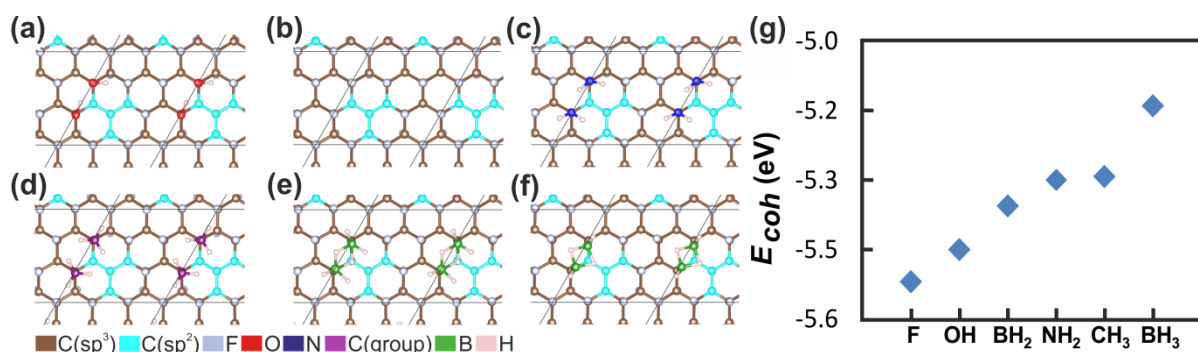


**Fig. S2** Structures of (a)  $C_{18}(OH)_2F_{12}$ , (b)  $C_{18}F_{14}$ , (c)  $C_{18}(NH_2)_2F_{12}$ , (d)  $C_{18}(CH_3)_2F_{12}$ , (e)  $C_{18}(BH_3)_2F_{12}$ , and (f)  $C_{18}(BH_2)_2F_{12}$  with embedded trimethylenemethane motifs.  $sp^3$  carbon atoms are shown in brown, and  $sp^2$  carbon atoms in cyan. The G(SH)F was unstable: the -SH groups desorbed from the graphene lattice. The size of computational cell is indicated by solid lines. (g) Energetic stability of the G(X)F derivatives with embedded trimethylenemethane motifs in terms of cohesive energy per atom.

**Table S2** Average bond distance (Å) between functional groups and  $sp^3$  carbon atom below of  $C_{18}(X)_4F_6$  with embedded *m*-xylylene and  $C_{18}(X)_2F_{12}$  with embedded trimethylenemethane motifs

Bond distance (Å)	OH	NH <sub>2</sub>	CH <sub>3</sub>	BH <sub>3</sub>	BH <sub>2</sub>	F
$C_{18}(X)_4F_6$	1.44	1.48	1.58	1.66	1.66	1.41
$C_{18}(X)_2F_{12}$	1.43	1.47	1.60	1.68	1.67	1.40

**Table S3** Charge transfer expressed as Bader charges of functional groups of G(X)F

Bader charges ( $e^-$ )	OH	NH <sub>2</sub>	CH <sub>3</sub>	BH <sub>3</sub>	BH <sub>2</sub>	F
$C_{18}(X)_4F_6$	-0.43	-0.63	-0.04	-	-	-0.57
$C_{18}(X)_2F_{12}$	-0.41	-0.59	-0.02	1.33	1.21	-0.56

**Table S4** Magnetic properties of G(X)F derivatives

Spin number $S$	OH	NH <sub>2</sub>	CH <sub>3</sub>	BH <sub>3</sub>	BH <sub>2</sub>	F
$C_{18}(X)_4F_6$	1.00	1.00	1.00	0.00	0.00	1.00
$C_{18}(X)_2F_{12}$	1.00	1.00	1.00	1.00	1.00	1.00

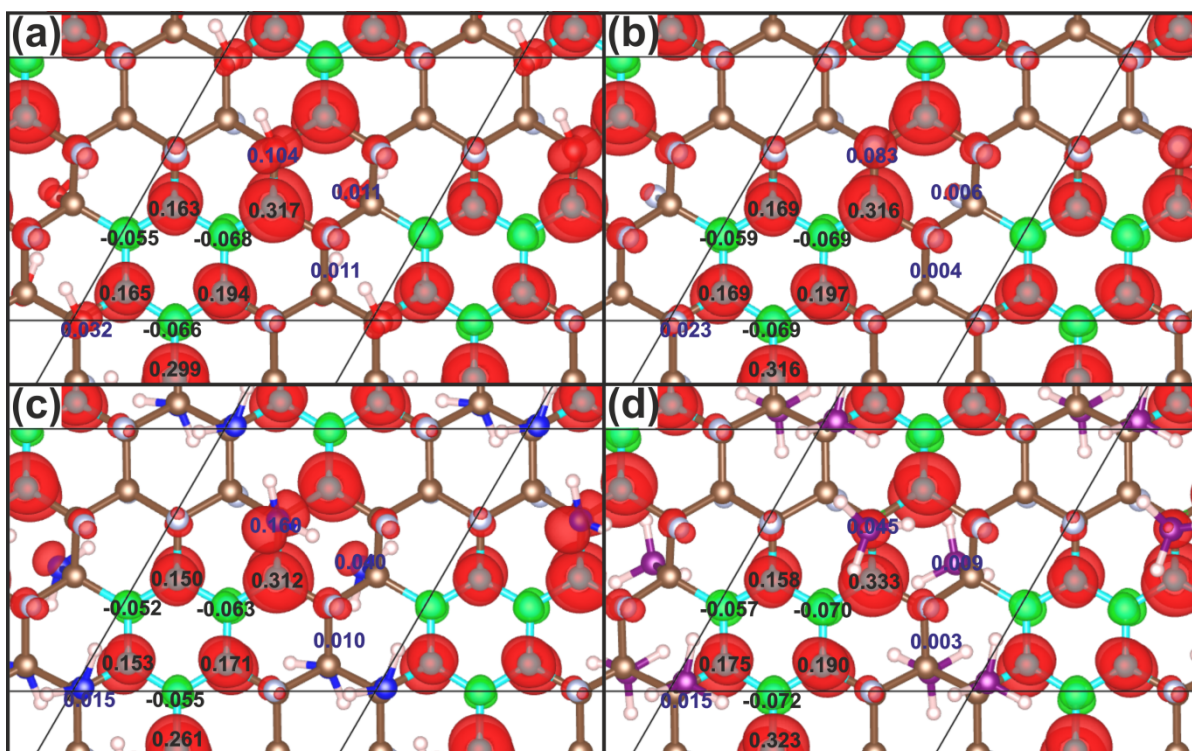


**Fig. S3** Spin density distribution plot of G(X)F derivatives with embedded MX motif (FM phase); (a)  $C_{18}(OH)_4F_6$ , (b)  $C_{18}F_{10}$ , (c)  $C_{18}(NH_2)_4F_6$ , (d)  $C_{18}(CH_3)_4F_6$ .  $sp^3$  carbon atoms are shown in brown and  $sp^2$  carbon atoms in turquoise. Red/green colored spin-density corresponds to positive/negative magnetic moments. Isovalue  $5 \cdot 10^{-3} \text{ e}\text{\AA}^{-3}$ . Numbers denote local magnetic moments. Cf. Fig. S2.

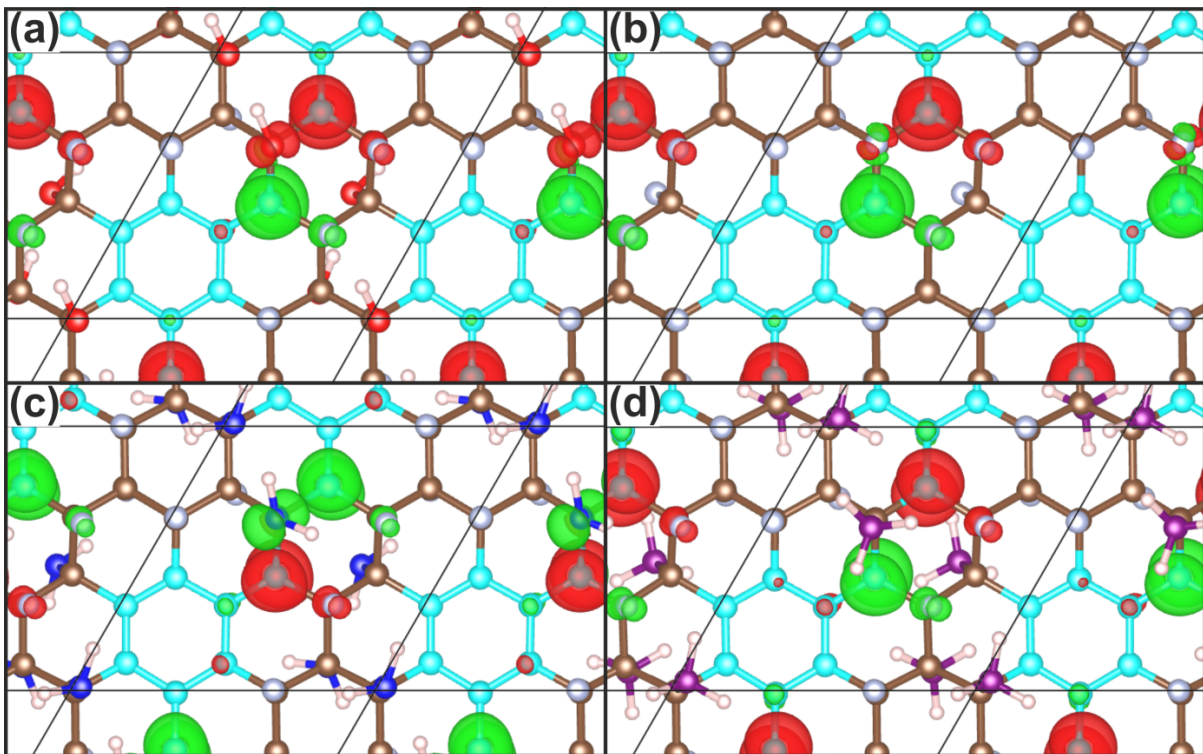


**Fig. S4** Spin density distribution plots of G(X)F derivatives with embedded MX motifs (AFM phase).

(a)  $C_{18}(OH)_4F_6$ , (b)  $C_{18}F_{10}$ , (c)  $C_{18}(NH_2)_4F_6$ , (d)  $C_{18}(CH_3)_4F_6$ .  $sp^3$  carbon atoms are shown in brown and  $sp^2$  carbon atoms in turquoise. Red/green colored spin-densities correspond to positive/negative magnetic moments.

Isovalue  $5 \cdot 10^{-3} \text{ e}\text{\AA}^{-3}$ . Cf. Fig. S2.

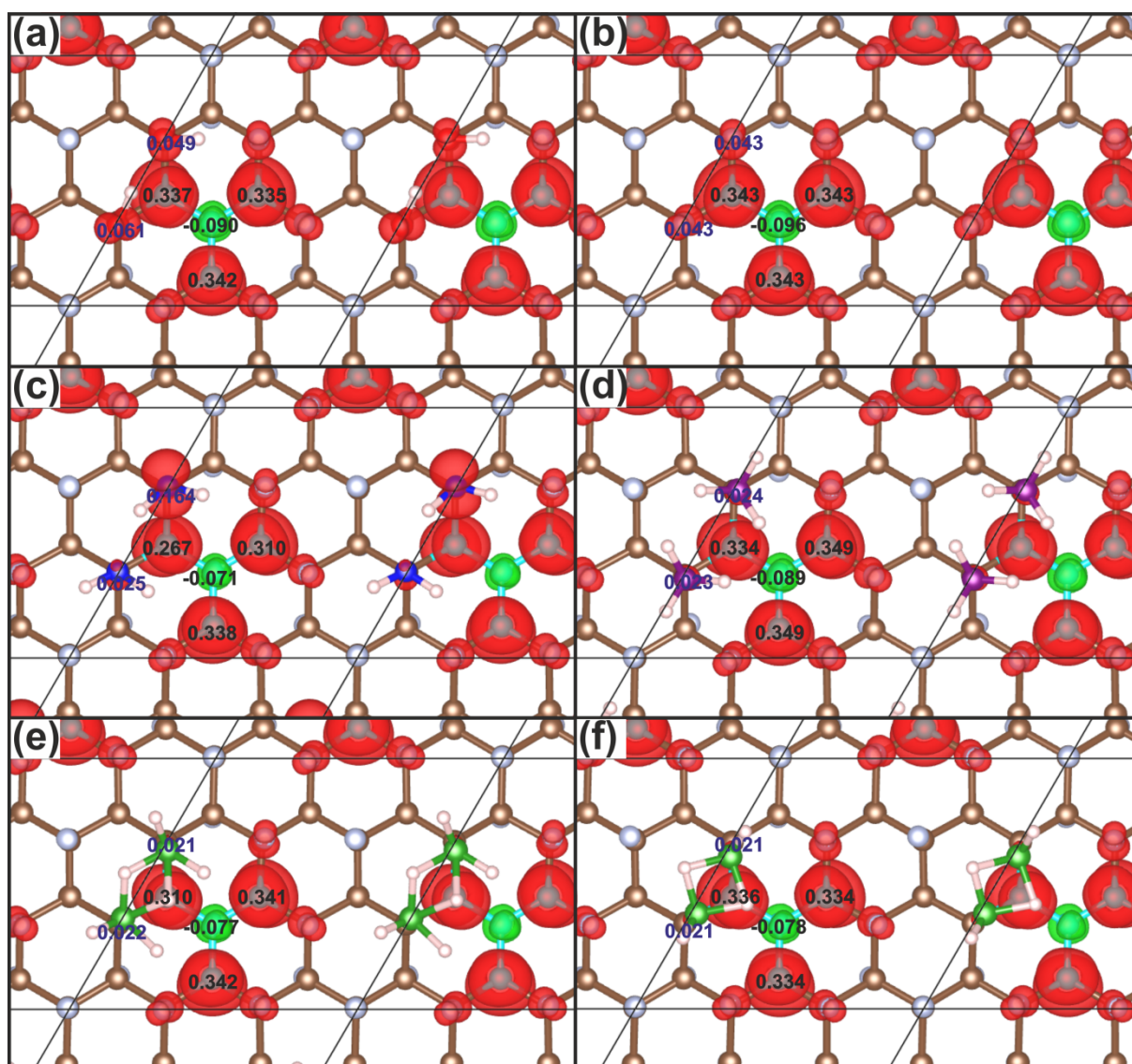


**Fig. S5** Spin density distribution plots of G(X)F derivatives with embedded trimethylenemethane motifs (FM phase). (a)  $C_{18}(OH)_2F_{12}$ , (b)  $C_{18}F_{14}$ , (c)  $C_{18}(NH_2)_2F_{12}$ , (d)  $C_{18}(CH_3)_2F_{12}$ , (e)  $C_{18}(BH_3)_2F_{12}$ , (f)  $C_{18}(BH_2)_2F_{12}$ .  $sp^3$  carbon atoms are shown in brown and  $sp^2$  carbon atoms in turquoise. Red/green colored spin-densities correspond to positive/negative magnetic moments. Isovalue  $5 \cdot 10^{-3} \text{ e}\text{\AA}^{-3}$ . Numbers denote local magnetic moments. Cf. Fig. S2.

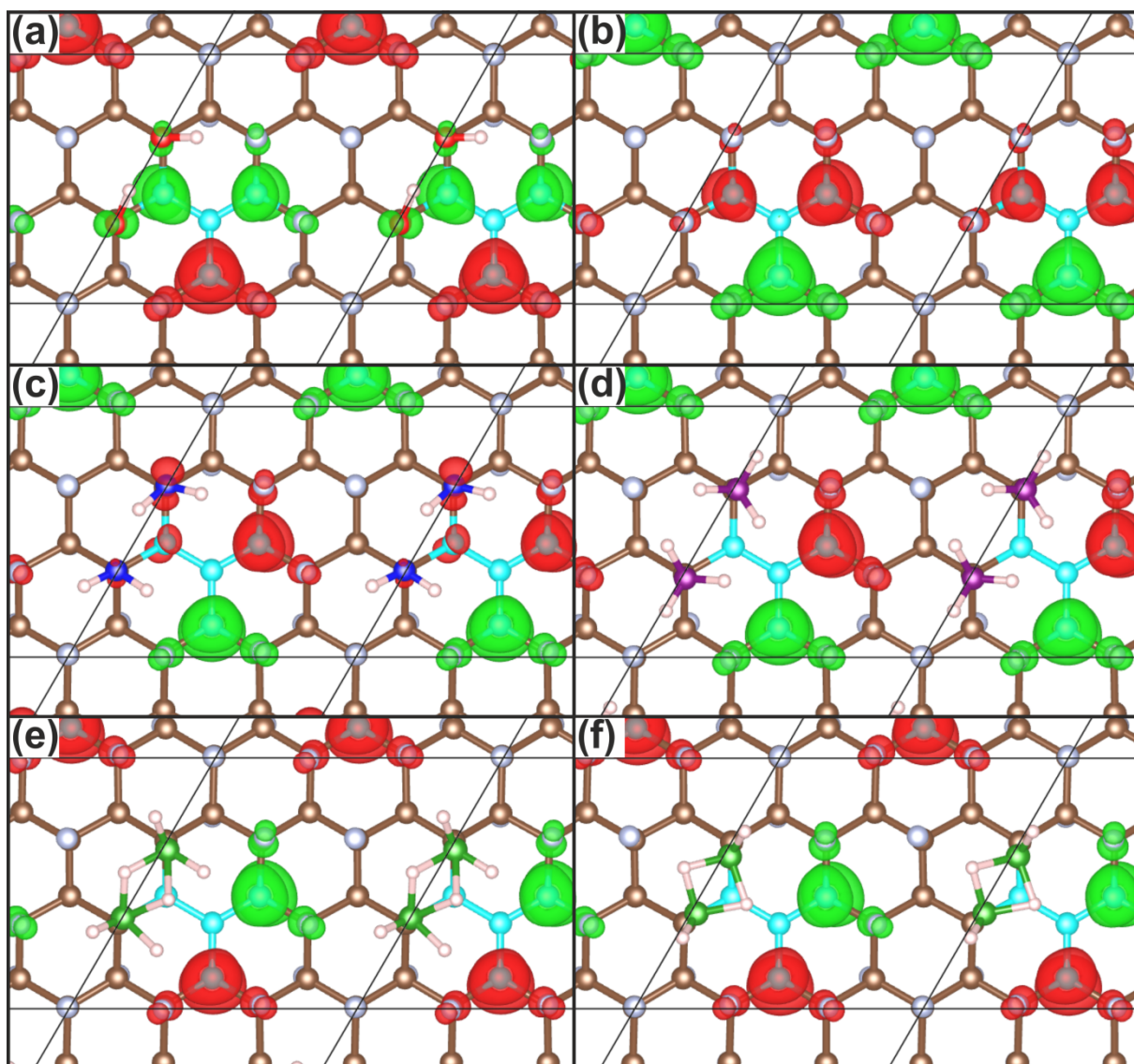


**Fig. S6** Spin density distribution plots of G(X)F derivatives with embedded trimethylenemethane motifs (AFM phase). (a)  $C_{18}(OH)_2F_{12}$ , (b)  $C_{18}F_{14}$ , (c)  $C_{18}(NH_2)_2F_{12}$ , (d)  $C_{18}(CH_3)_2F_{12}$ , (e)  $C_{18}(BH_3)_2F_{12}$ , (f)  $C_{18}(BH_2)_2F_{12}$ .  $sp^3$  carbon atoms are shown in brown and  $sp^2$  carbon atoms in turquoise. Red/green colored spin-densities correspond to positive/negative magnetic moments. Isovalue  $5 \cdot 10^{-3} e\text{\AA}^{-3}$ . Cf. Fig. S2.

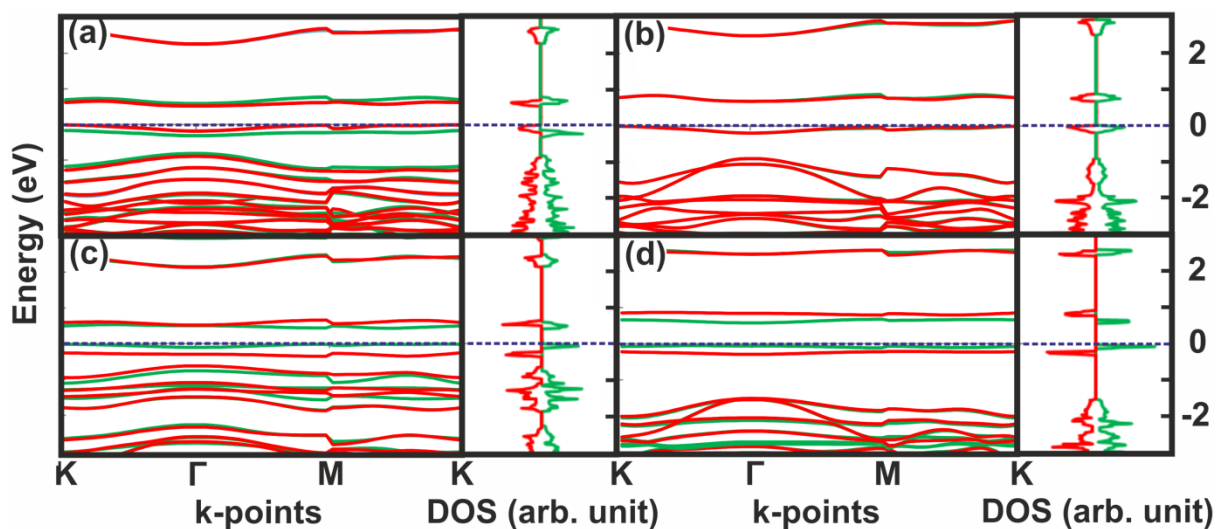


**Fig. S7** Density of states (DOS) and bandstructure (AFM phase). (a)  $C_{18}(\text{OH})_4\text{F}_6$ , (b)  $C_{18}\text{F}_{10}$ , (c)  $C_{18}(\text{NH}_2)_4\text{F}_6$ , (d)  $C_{18}(\text{CH}_3)_4\text{F}_6$ . Red/green lines correspond to spin up/down bands. The Fermi level is set to zero.

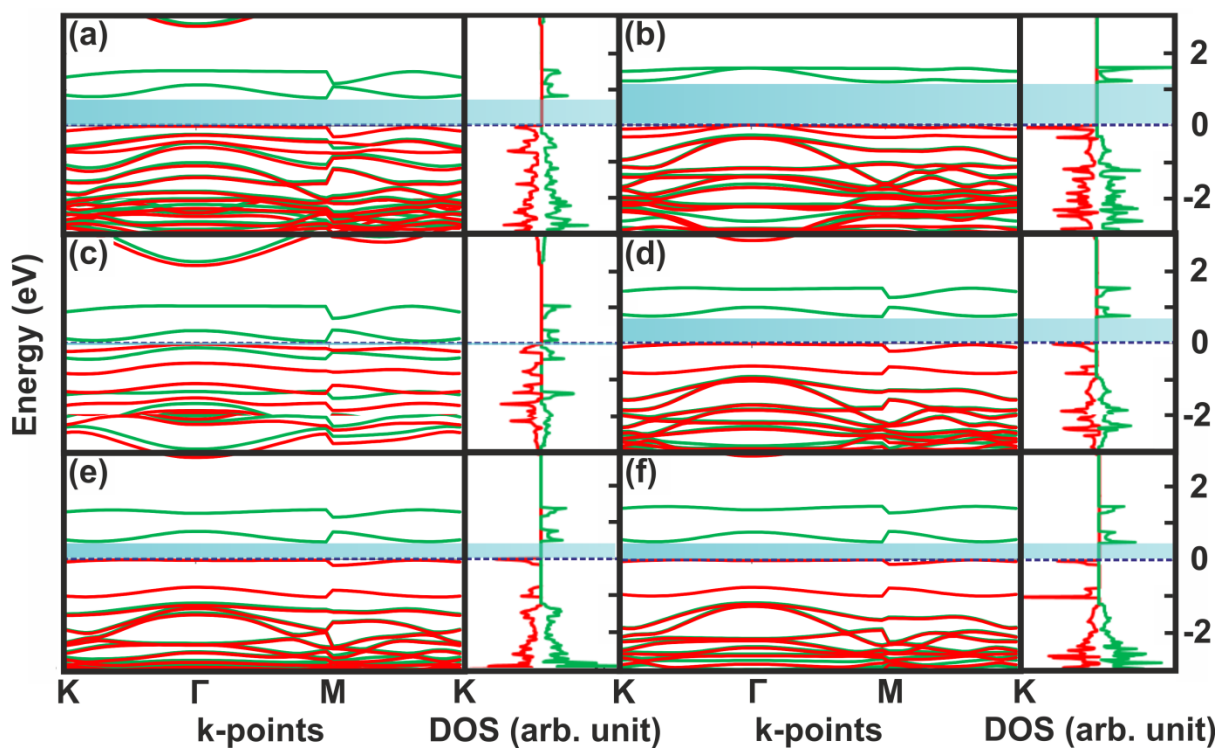


**Fig. S8** Density of states (DOS) and bandstructure (FM phase). (a)  $C_{18}(\text{OH})_2\text{F}_{12}$ , (b)  $C_{18}\text{F}_{14}$ , (c)  $C_{18}(\text{NH}_2)_2\text{F}_{12}$ , (d)  $C_{18}(\text{CH}_3)_2\text{F}_{12}$ , (e)  $C_{18}(\text{BH}_3)_2\text{F}_{12}$ , (f)  $C_{18}(\text{BH}_2)_2\text{F}_{12}$ . Red/green lines correspond to spin up/down bands. The Fermi level is set to zero. The light blue bar represents the spin-flip gap.

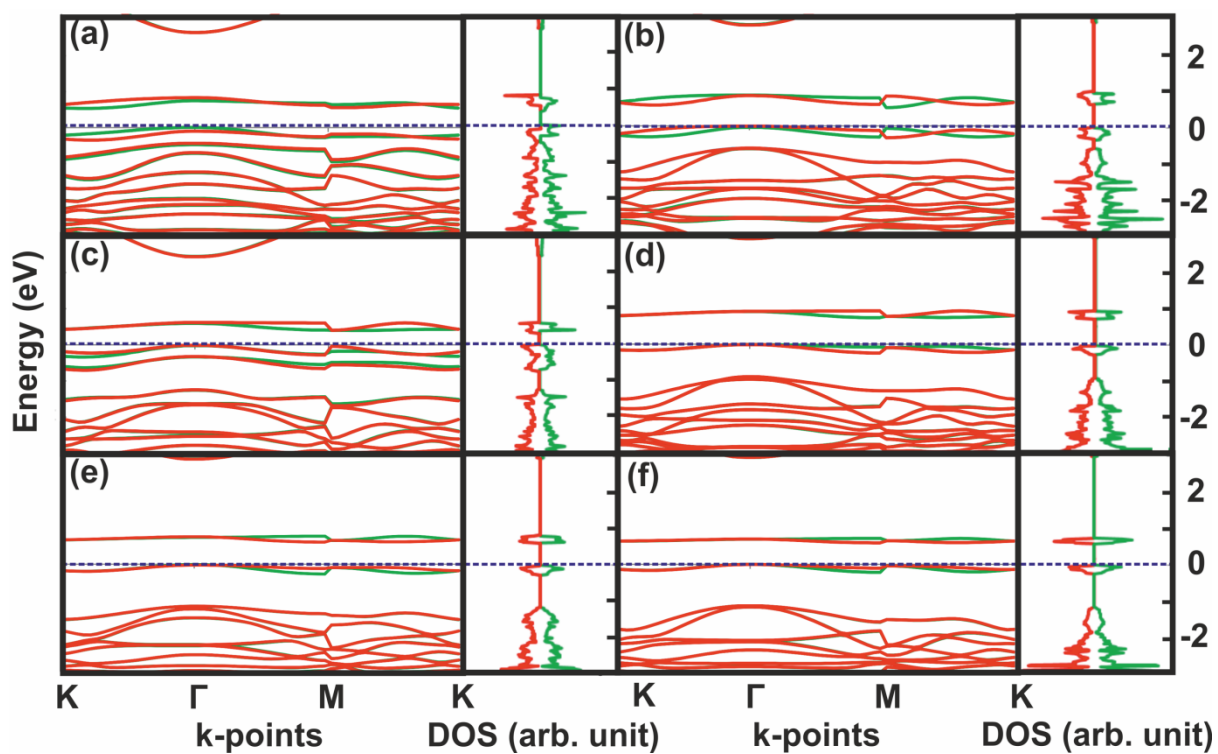


**Fig. S9** Density of states (DOS) and bandstructure (AFM phase). (a)  $C_{18}(\text{OH})_2\text{F}_{12}$ , (b)  $C_{18}\text{F}_{14}$ , (c)  $C_{18}(\text{NH}_2)_2\text{F}_{12}$ , (d)  $C_{18}(\text{CH}_3)_2\text{F}_{12}$ , (e)  $C_{18}(\text{BH}_3)_2\text{F}_{12}$ , (f)  $C_{18}(\text{BH}_2)_2\text{F}_{12}$ . Red/green lines correspond to spin up/down bands. The Fermi level is set to zero.

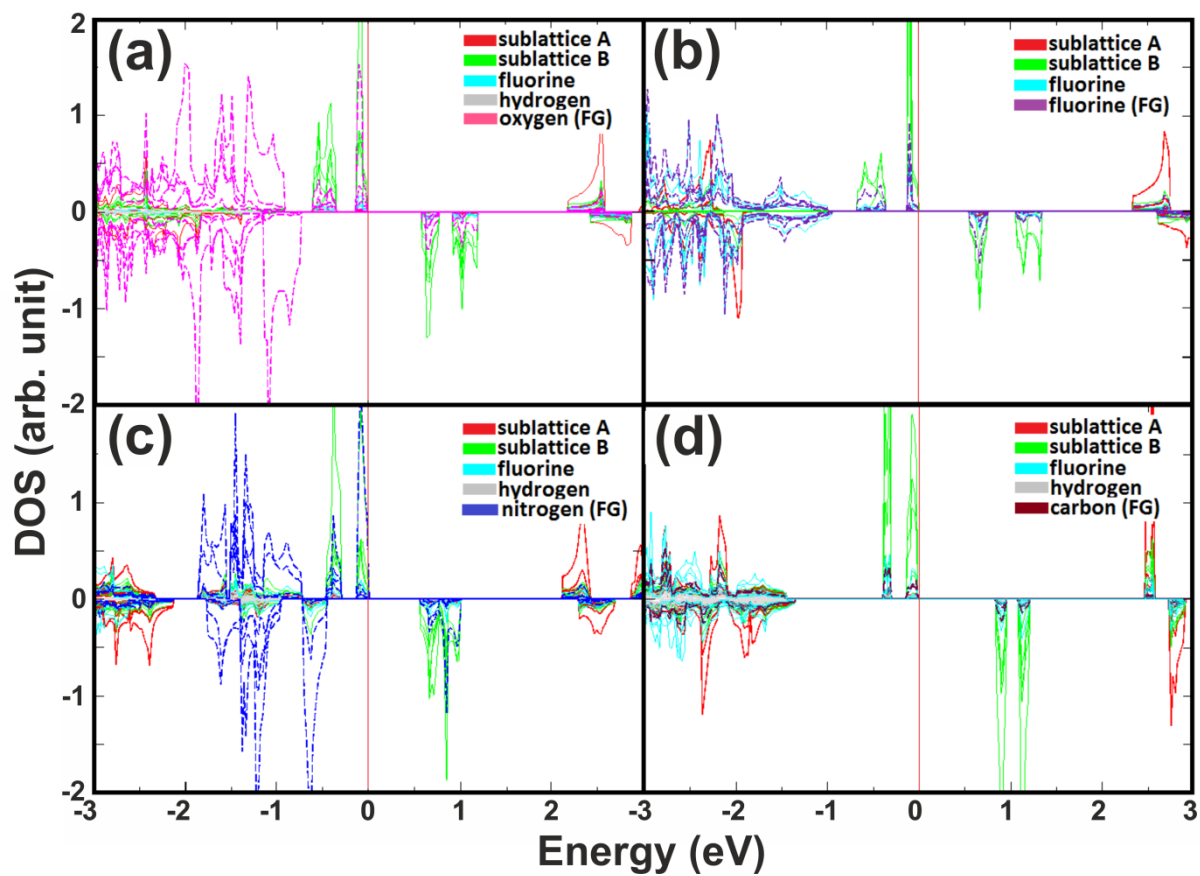


**Fig. S10** Atom-resolved DOS plots of G(X)F with *m*-xylylene motifs (FM phase). (a)  $C_{18}(OH)_4F_6$ , (b)  $C_{18}F_{10}$ , (c)  $C_{18}(NH_2)_4F_6$ , (d)  $C_{18}(CH_3)_4F_6$ . The Fermi level is set to zero.

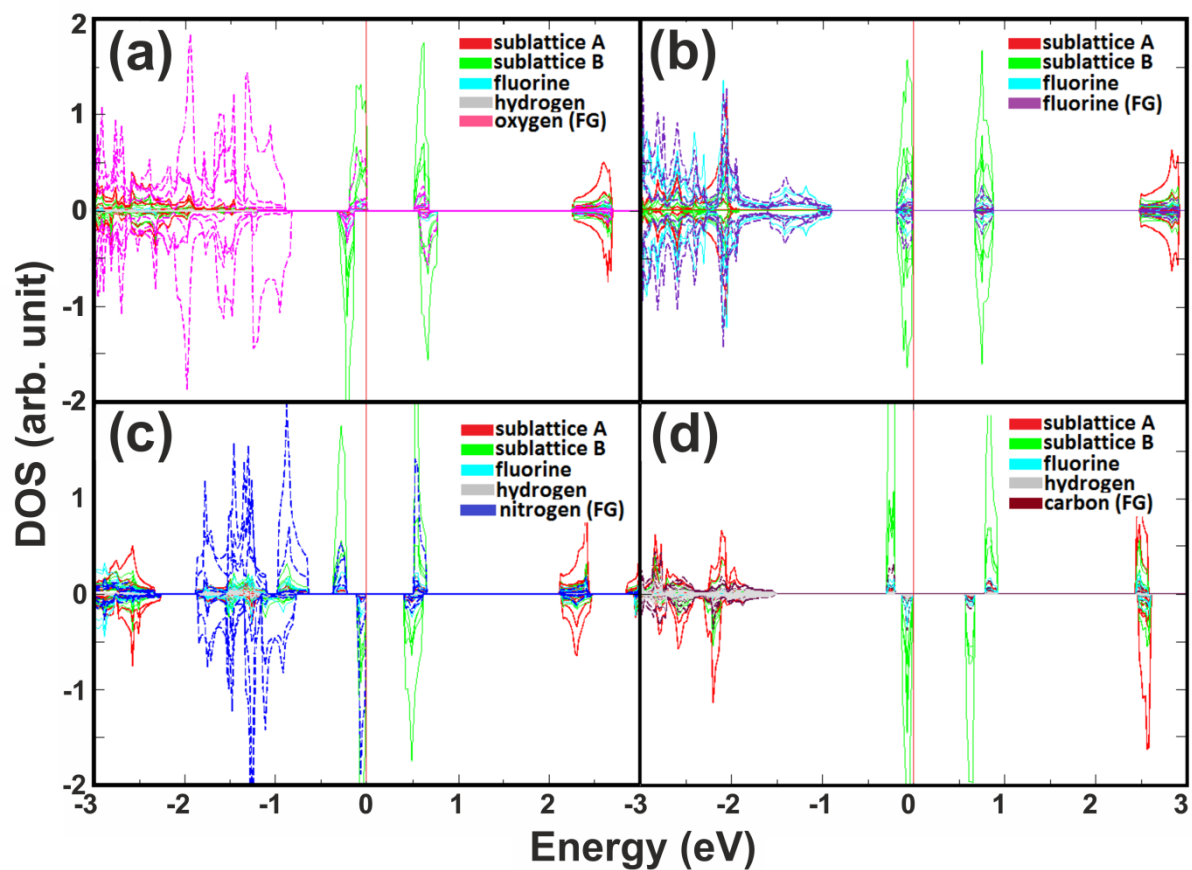
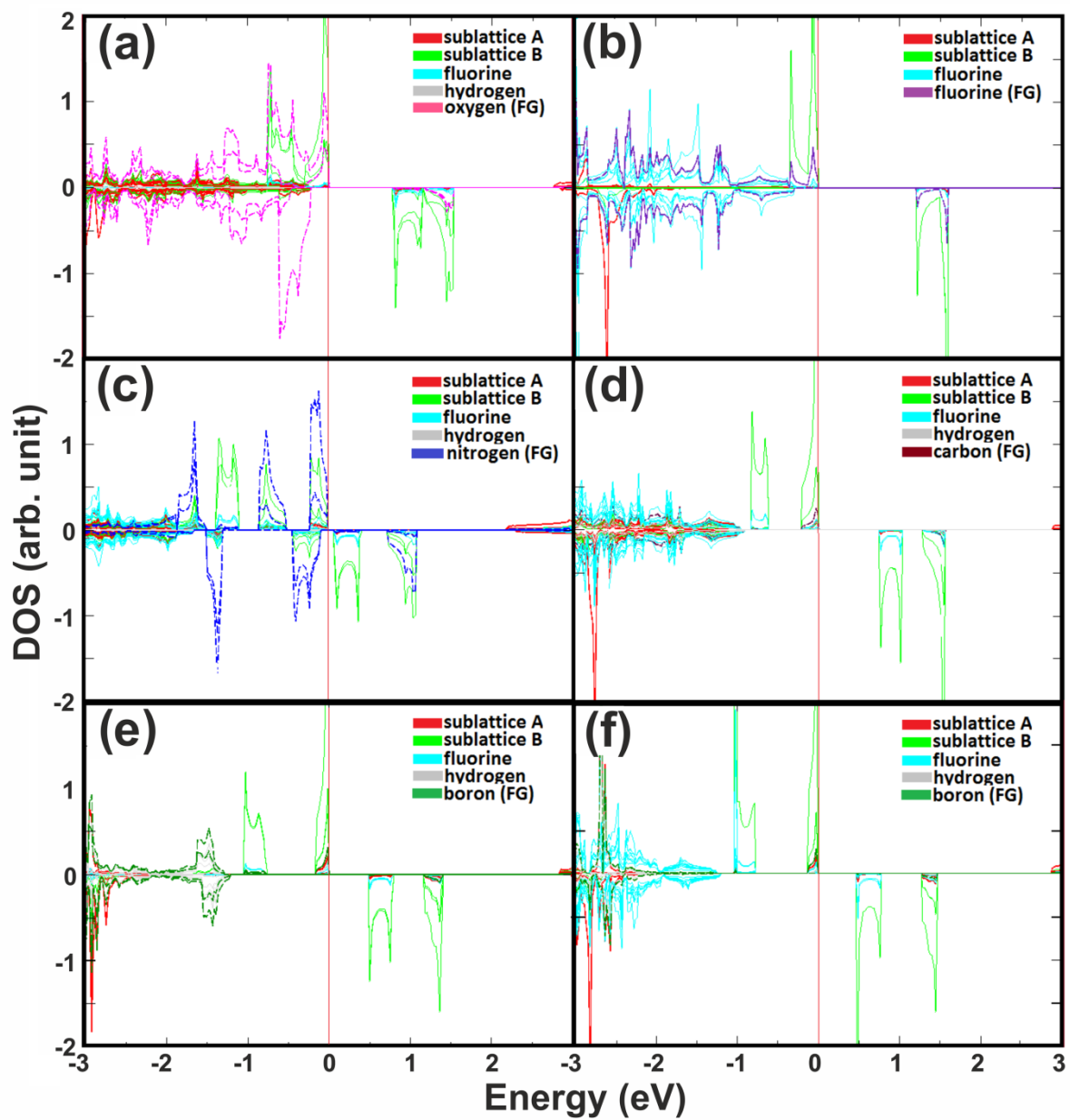
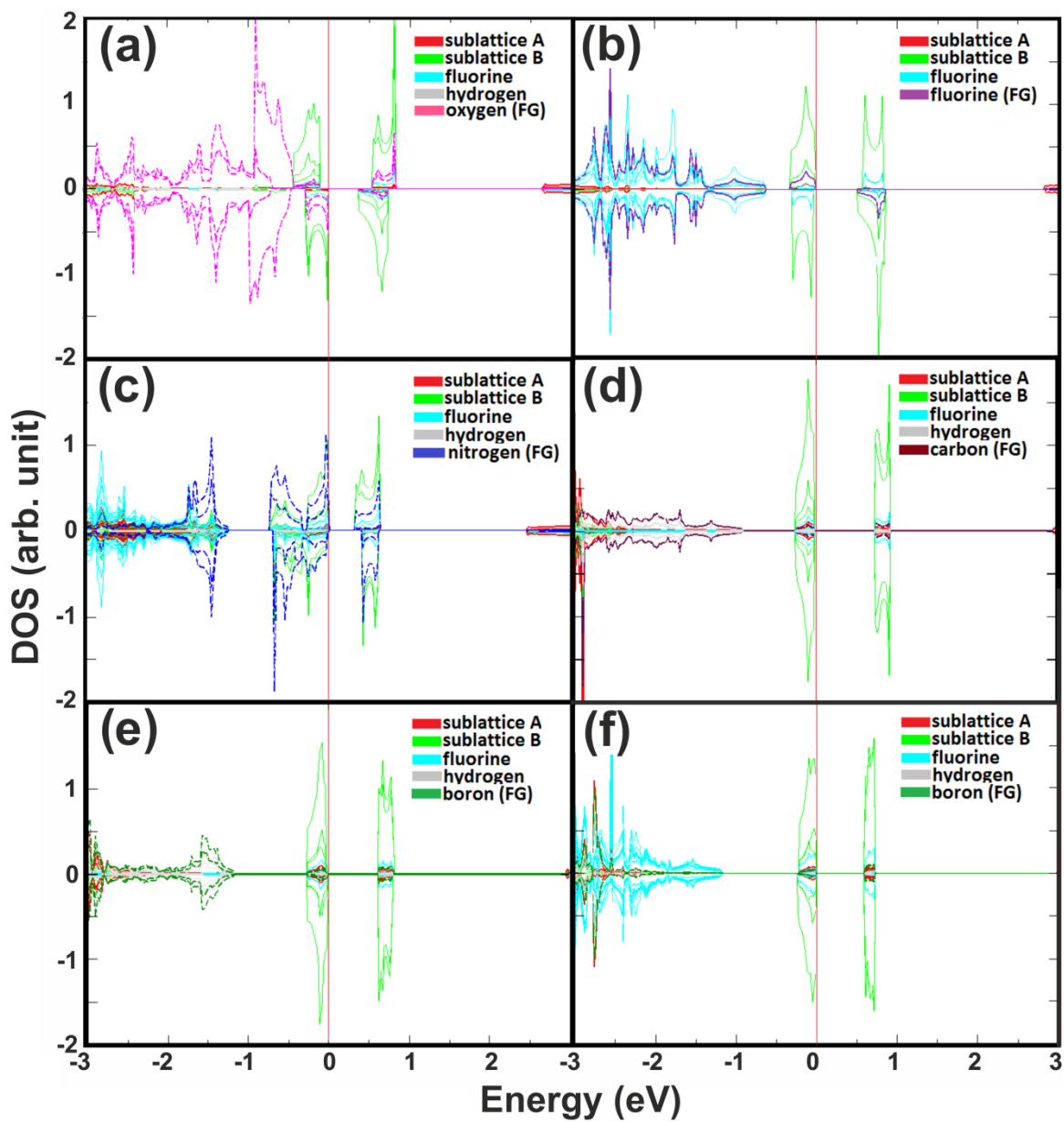


Fig. S11 Atom-resolved DOS plots of  $G(X)F$  with *m*-xylylene motifs (AFM phase). (a)  $C_{18}(OH)_4F_6$ , (b)  $C_{18}F_{10}$ , (c)  $C_{18}(NH_2)_4F_6$ , (d)  $C_{18}(CH_3)_4F_6$ . The Fermi level is set to zero.



**Fig. S12** Atom-resolved DOS plots of G(X)F with trimethylenemethane motifs (FM phase). (a)  $C_{18}(OH)_2F_2$ , (b)  $C_{18}F_{14}$ , (c)  $C_{18}(NH_2)_2F_{12}$ , (d)  $C_{18}(CH_3)_2F_{12}$ , (e)  $C_{18}(BH_3)_2F_{12}$ , (f)  $C_{18}(BH_2)_2F_{12}$ . The Fermi level is set to zero.



**Fig. S13** Atom-resolved DOS plots of G(X)F with trimethylenemethane motifs (AFM phase). (a)  $C_{18}(OH)_2F_2$ , (b)  $C_{18}F_{14}$ , (c)  $C_{18}(NH_2)_2F_{12}$ , (d)  $C_{18}(CH_3)_2F_{12}$ , (e)  $C_{18}(BH_3)_2F_{12}$ , (f)  $C_{18}(BH_2)_2F_{12}$ . The Fermi level is set to zero.

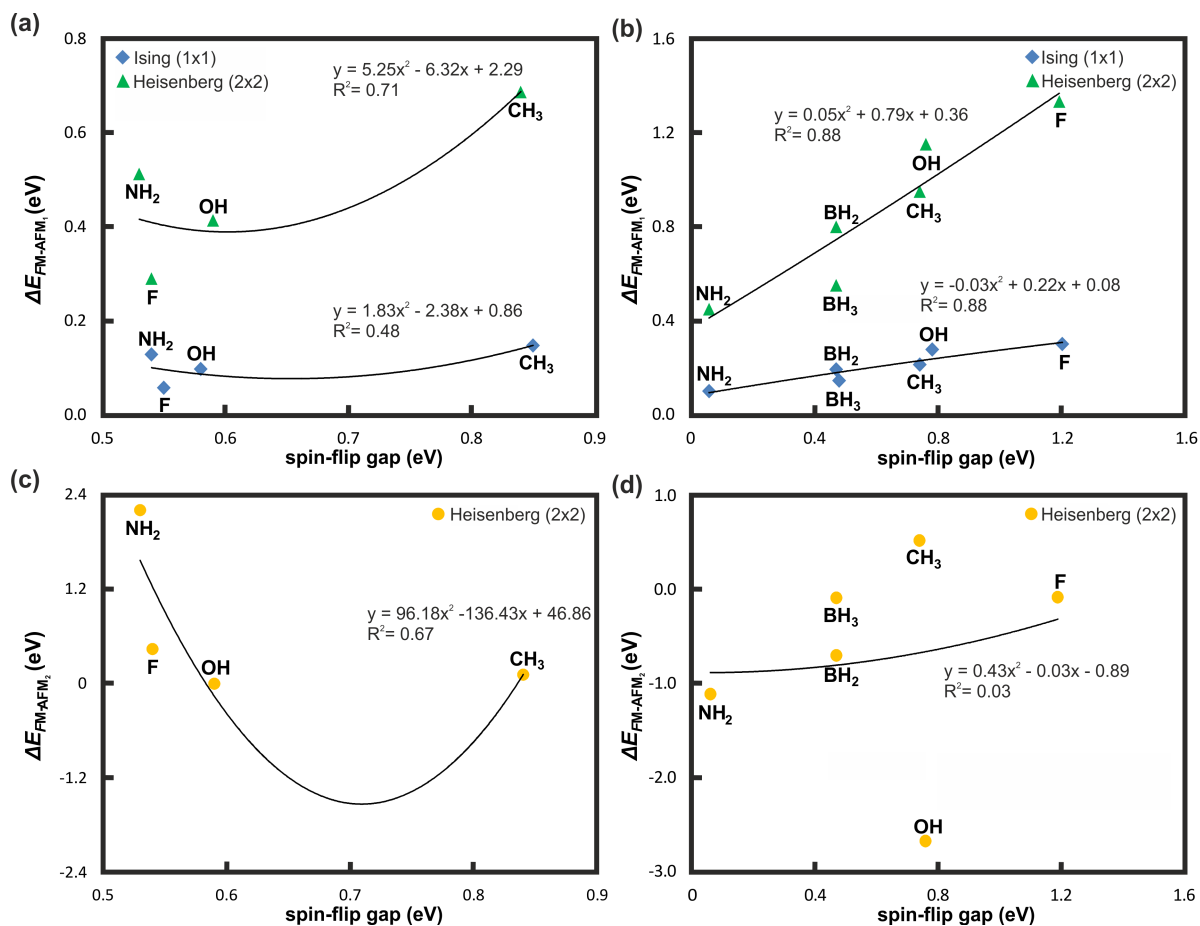


**Fig. S14**  $\Delta E_{FM-AFM}$  as a function of the spin-flip gap between the occupied spin-up and empty spin-down channels of G(X)F derivatives: (a) MX motifs (blue: 1 x 1 cell, Ising model and green: 2 x 2 cell, Heisenberg model with the AFM<sub>1</sub> phase), (b) the same as (a) for TMM motifs, (c) MX motifs for 2 x 2 cell and the Heisenberg model with the AFM<sub>2</sub> phase, and (d) the same as (c) for TMM motifs. Cf. Fig. S17.

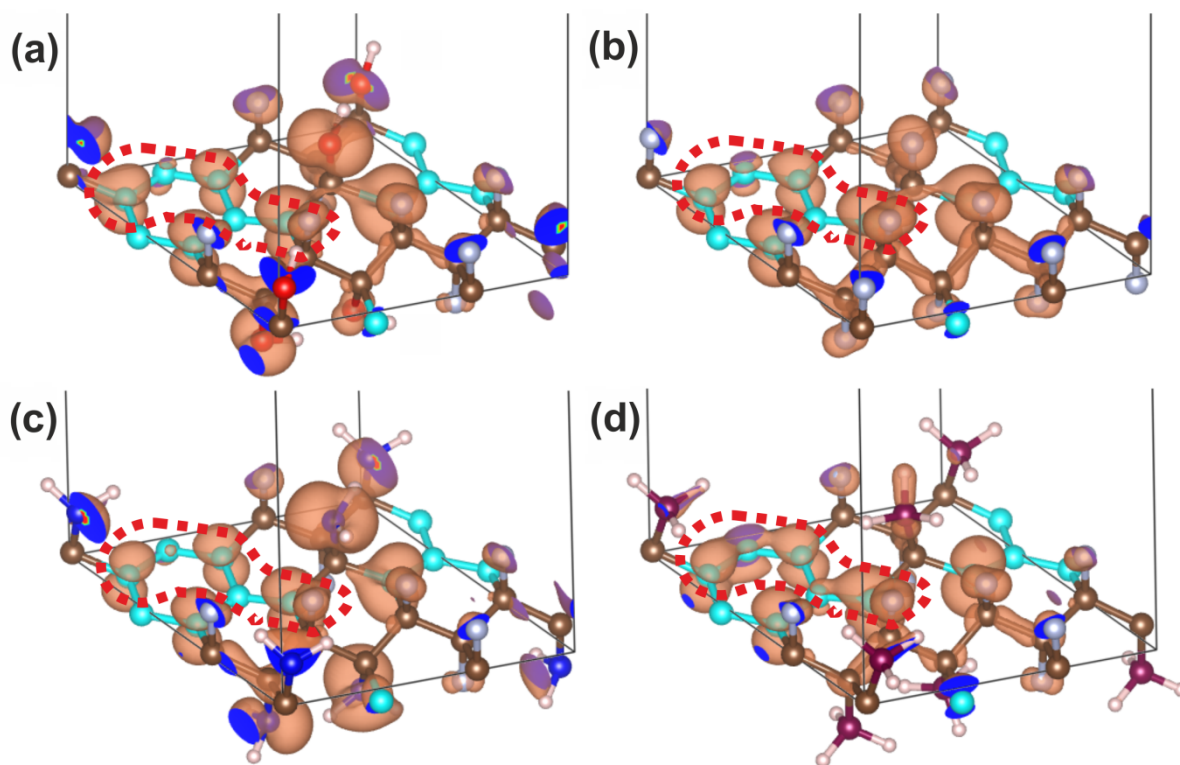


**Fig. S15** Partial charge density plots of G(X)F derivatives with *m*-xylylene motifs. (a)  $C_{18}(OH)_4F_6$ , (b)  $C_{18}F_{10}$ , (c)  $C_{18}(NH_2)_4F_6$ , (d)  $C_{18}(CH_3)_4F_6$ .  $sp^3$  carbon atoms in brown and  $sp^2$  carbon atoms in turquoise. Isovalue  $1.5 \cdot 10^{-2} e\text{\AA}^{-3}$ .

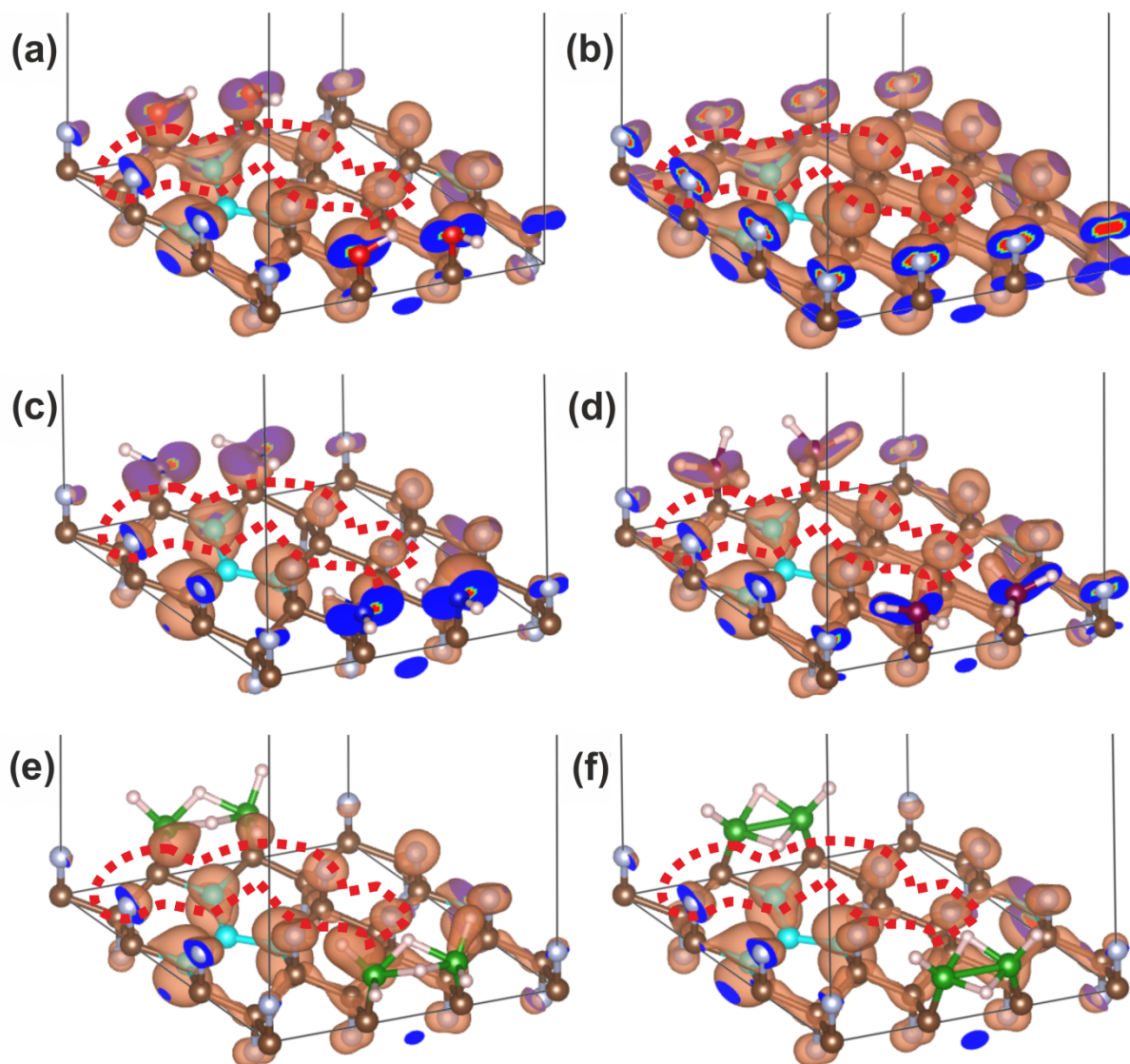


**Fig. S16** Partial charge density plots of G(X)F derivatives with trimethylenemethane motifs. (a)  $C_{18}(OH)_2F_{12}$ , (b)  $C_{18}F_{14}$ , (c)  $C_{18}(NH_2)_2F_{12}$ , (d)  $C_{18}(CH_3)_2F_{12}$ , (e)  $C_{18}(BH_3)_2F_{12}$ , (f)  $C_{18}(BH_2)_2F_{12}$ .  $sp^3$  carbon atoms in brown, and  $sp^2$  carbon atoms in turquoise. Isovalue  $1.5 \cdot 10^{-2} e\text{\AA}^{-3}$ .

**Table S5** The exchange coupling  $J$  (eV) and the magnetic transition temperature  $T$  (K) calculated using the Ising expression and mean-field expression of G(X)F derivatives with embedded *m*-xylylene and trimethylenemethane motifs.

	Ising model				Mean-field	
	$J_{\text{FM-AFM}}$	$J_{\text{FM-NM}}$	$T_{\text{FM-AFM}}$	$T_{\text{FM-NM}}$	$T_{\text{FM-AFM1}}$	$T_{\text{FM-AFM2}}$
<b>C<sub>18</sub>F<sub>10</sub></b>	0.0095	0.0268	41.98	118.09	112.05	168.57
<b>C<sub>18</sub>(OH)<sub>4</sub>F<sub>6</sub></b>	0.0162	0.0382	71.42	168.31	159.95	0.99
<b>C<sub>18</sub>(NH<sub>2</sub>)<sub>4</sub>F<sub>6</sub></b>	0.0214	0.0594	94.13	261.80	198.07	850.96
<b>C<sub>18</sub>(CH<sub>3</sub>)<sub>4</sub>F<sub>6</sub></b>	0.0246	0.0832	108.22	366.55	265.47	42.55
<b>C<sub>18</sub>F<sub>14</sub></b>	0.0500	0.0959	220.09	422.56	859.30	54.24
<b>C<sub>18</sub>(OH)<sub>2</sub>F<sub>12</sub></b>	0.0460	0.0802	202.47	353.45	742.06	1727.17
<b>C<sub>18</sub>(NH<sub>2</sub>)<sub>2</sub>F<sub>12</sub></b>	0.0164	0.0361	72.26	159.21	288.65	719.02
<b>C<sub>18</sub>(CH<sub>3</sub>)<sub>2</sub>F<sub>12</sub></b>	0.0353	0.0805	155.39	354.85	611.89	334.17
<b>C<sub>18</sub>(BH<sub>3</sub>)<sub>2</sub>F<sub>12</sub></b>	0.0239	0.0557	105.46	245.28	354.24	58.29
<b>C<sub>18</sub>(BH<sub>2</sub>)<sub>2</sub>F<sub>12</sub></b>	0.0318	0.0626	140.19	275.90	514.88	453.96

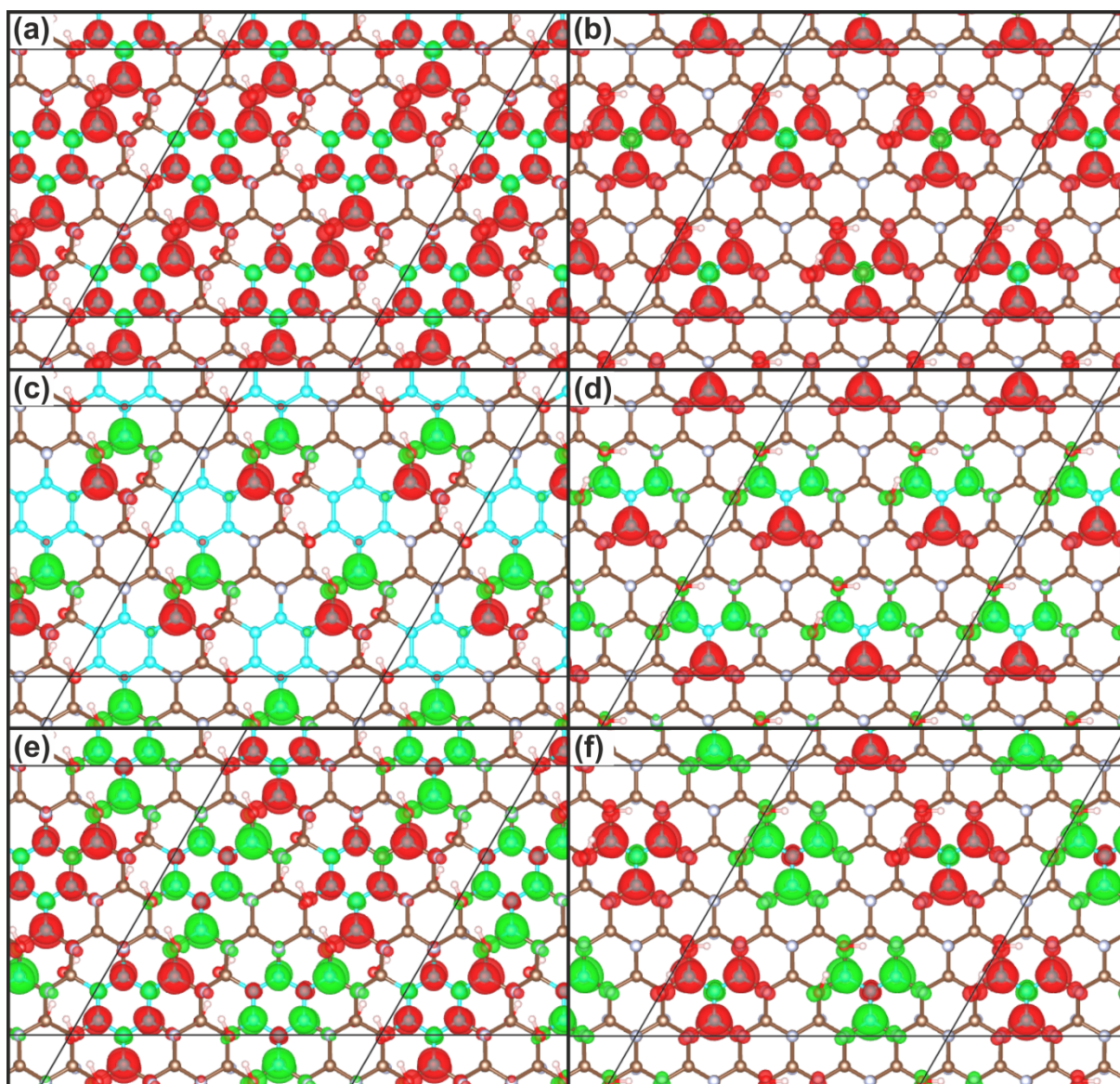


**Fig. S17** Spin density distribution plots of G(X)F derivatives for 2 x 2 cell. (a) FM phase (MX motifs), (b) FM phase (TMM motifs), (c) AFM<sub>1</sub> phase (MX motif), (d) AFM<sub>1</sub> phase (TMM motif), (e) AFM<sub>2</sub> phase (MX motif), (f) AFM<sub>2</sub> (TMM) motif.  $sp^3$  carbon atoms are shown in brown and  $sp^2$  carbon atoms in turquoise. Red/green colored spin-densities correspond to positive/negative magnetic moments. Isovalue  $5 \cdot 10^{-3} \text{ e}\text{\AA}^{-3}$ . Cf. Fig. S2.

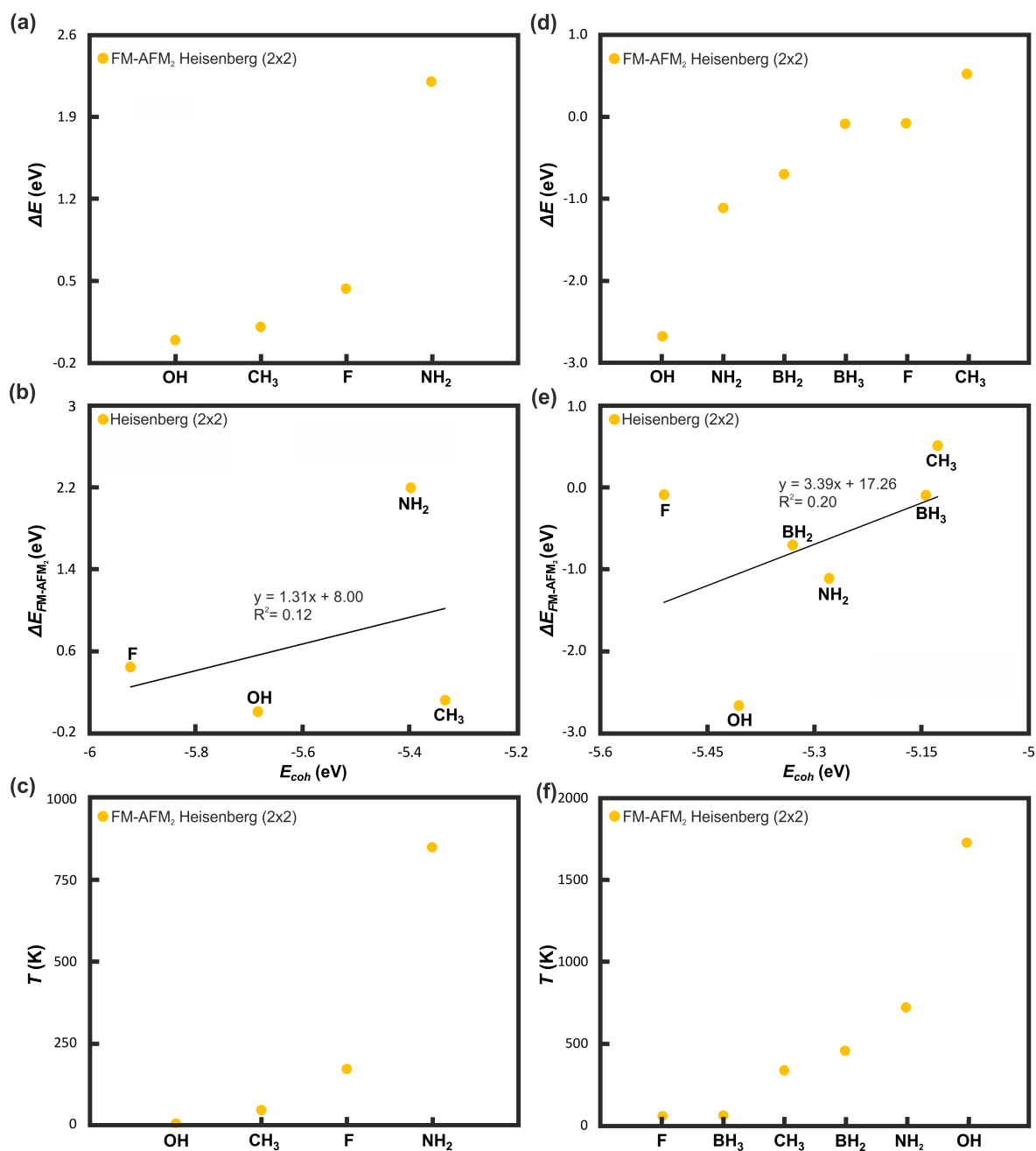


**Fig. 18** (a-b, d-e) Energy difference  $\Delta E$  between the FM state and the AFM<sub>2</sub> state (cf. Fig. S17e,f), (b, e)  $\Delta E_{\text{FM-AFM}_2}$  of G(X)F derivatives as a function of their  $E_{\text{coh}}$  values, and (c, f) the theoretical transition temperature calculated with the Heisenberg model for G(X)F derivatives with embedded m-xylylene (a-c) and trimethylenemethane motif (d-f).